LETTER

The solubility and oxidation state of nickel in silicate melt at low oxygen fugacities: Results using a mechanically assisted equilibration technique

D. B. DINGWELL,[1] H. ST.C. O'NEILL,[1] W. ERTEL,[1] and B. SPETTEL[2]

[1]Bayerisches Geoinstitut, Universität Bayreuth, 95440 Bayreuth, Germany
[2]Max-Planck-Institut für Chemie, Postfach 3060, 55020 Mainz, Germany

Abstract—The solubility of Ni in a silicate melt has been measured using a new, mechanically assisted equilibration technique over a wide range of controlled f_{O_2} values. The melt composition corresponds to the 1 atm eutectic in the system $CaAl_2Si_2O_8$–$CaMgSi_2O_6$ + 10 wt% CaO. The experiments were performed at 1300°C and over an f_{O_2} range of $10^{-8.5}$ to $10^{-13.75}$, and over a temperature range of 1270 to 1390°C at a constant gas mixing ratio ($CO_2/CO = 1:1$). The experiment consists of a sample of melt contained within a crucible of Ni metal and held in a 1 atm gas mixing furnace. A Ni spindle is entered into the sample from above and continuously rotated at a constant angular velocity using a viscometer head. The stirring of the sample serves to accelerate the approach to equilibrium between the liquid sample and the metal crucible (and spindle). This arrangement allows relatively rapid equilibration of Ni content following changes to higher or lower f_{O_2} values. Samples of the melt may be taken at any time for analysis, and thus the equilibrium solubility of Ni in the silicate melt may be determined from unambiguous experimental reversals. The Ni contents of samples, analysed both by INAA and by ICP–AES, range from 25 to 5300 ppm.

The data presented in this paper indicate that the oxidation state of Ni in the investigated melt is Ni^{2+} over the entire range of f_{O_2} investigated. This conclusion contrasts with recent reports in the literature of an inflection in the f_{O_2} dependence of Ni solubility, which has been interpreted as solution of neutral Ni at low f_{O_2} (MORSE et al., 1991; COLSON, 1992; EHLERS et al., 1992). We also present data for the temperature dependence of Ni solubility in the investigated melt. The solubility decreases with increasing temperature at constant f_{O_2}. The present results are in good agreement with the metal-loop-equilibration experiments reported by HOLZHEID et al. (1994).

INTRODUCTION

THERE HAVE RECENTLY BEEN several claims that substantial amounts (i.e., hundreds of parts per million) of neutral, zero-valent Ni (Ni^0) dissolve in silicate melts (COLSON, 1992; EHLERS et al., 1992; MORSE et al., 1991). The geochemical implications of such a hypothesis are considerable: they include an explanation for the overabundance of Ni in the Earth's mantle (COLSON, 1992); and incompatible-element behavior of Ni at low (e.g., typical lunar) f_{O_2} (STEELE et al., 1992). In addition, unless Ni is totally anomalous, the postulated large zero-valent solubility of Ni implies that the zero-valent solubility of many other siderophile elements may greatly exceed their mantle abundances, and thus dominate their high temperature geochemical properties.

To address the possibility of zero-valent Ni solubility at low f_{O_2} we have employed a new experimental strategy for the collection of metal solubility data as a function of silicate melt composition, temperature, and f_{O_2}. The method consists of equilibrating in a gas-mixing furnace a relatively large amount (100 g) of silicate melt, which is held in a crucible made from the metal of interest (e.g., here Ni). The melt is continuously stirred by a spindle of the same metal. The f_{O_2} of the experiment is controlled using conventional gas mixing techniques. Samples may be withdrawn from the cru-

cible for analysis at any time. The method permits the monitoring of changes in metal solubility as a time series after changing f_{O_2}, temperature, or melt composition. This provides a means by which attainment of equilibrium may be tested. Reversals of the equilibrium with respect to either oxygen fugacity or temperature may be performed, all during a single experimental run. The amount of sample withdrawn for analysis is of the order of 0.5 g, which permits the use of a wide variety of analytical methods, including those most suited for the determination of part per million abundances of the element in question. The result is a very precise determination of the dependence of Ni solubility on f_{O_2} over a wide range of these variables.

METHOD

Experimental

Several 80 g batches of a haplobasaltic composition in the system CaO–MgO–Al_2O_3–SiO_2 were prepared from analytical grade MgO, Al_2O_3, SiO_2, and $CaCO_3$, all chemicals were predried at 300°C ($CaCO_3$) or 1000°C. In addition, 100 g of a gel of similar composition was prepared by the usual methods containing 12.2 mg Sc_2O_3, so that the Sc could act as a monitor of analytical quality during the subsequent neutron activation analyses. 5 g of this gel mixture was added to each batch.

These mixtures were dried and fused in high density alumina crucibles (Friedrichsfeld AL23™) in a $MoSi_2$ box furnace at 1400°C for 30–60 min. The samples with crucibles were removed from the furnace and allowed to cool in air. The samples were then broken out of the alumina crucibles with a hammer and loaded as chips (25 g) into a Ni crucible at 1300°C and a low starting value of f_{O_2} (see Results section).

The experimental set-up for the solubility determinations is illustrated schematically in Fig. 1. The Ni crucible with sample rests on a hollow alumina pedestal in the hot zone of a vertical gas-mixing furnace within an alumina muffle tube, which is held at the top and the bottom by water cooling jackets.

For most of the work reported in this paper, the f_{O_2} was imposed using CO/CO_2 gas mixtures. CO and CO_2 gas flow rates were controlled using Tylan FC 280 S mass flow controllers (0–300 cm^3/s), operated electronically from a Tylan RO-7020/7021™ multi-channel read-out system. The f_{O_2} was continuously monitored for most of the experiment using a $SIRO_2$™ yttria-stabilized zirconia oxygen sensor, which was placed immediately below the crucible in the hot zone of the furnace. Slots are cut in the pedestal tube to facilitate gas circulation between sample and electrode. As a preliminary check of the system, the f_{O_2} in an empty crucible was checked using a second

oxygen sensor lowered from the top of the furnace, and compared with that measured by the permanent electrode below the crucible. The ranges of gas flow rates and f_{O_2} was determined for which no significant difference in f_{O_2} (log f_{O_2} within 0.03 log-bar units) between the two oxygen sensors was observable.

The temperature inside the muffle tube is measured on both sides of the oxygen electrode during the experiment using type B Pt/Rh thermocouples. The type B thermocouples were chosen over the more often used type S or R because they are mechanically stronger at higher temperature, and less liable to break. This is an important experimental consideration given the long duration of the experiment. The temperature typically varies by less than ±2°C over long periods of time (months) during gas mixing experiments.

To start the experiment, the Ni crucible is nearly filled with chips of prepared glass during an initial fusion in the crucible under low f_{O_2}, and a MgO collar is placed on the rim of the crucible to prevent accidental contact between the crucible and the spindle. We found during the early stages of the experiment that even brief contact between crucible and spindle causes them to stick fast together, necessitating the experiment to be cooled down to room temperature, and the crucible plus spindle to be removed and then separated. The Ni spindle is hung from a viscometer head (Brookfield RVTD) by a series of stainless steel segments, which pass into the muffle tube through a centered iris diaphragm in the top water-cooled jacket. The iris may be opened to the desired extent for access to the crucible during the initial loading and spindle insertion, and the subsequent sample extractions. During equilibration/stirring the iris is closed down to the size of the stainless steel stirring segment. The entire length of the Ni spindle and its Ni stem are kept within the controlled atmosphere in the alumina muffle tube, and never come into contact with air at elevated temperatures. Thus, surface oxidation is prevented.

The Ni spindle is lowered into the melt through the MgO collar and to a position a few millimeters above the Ni crucible floor using a lab stand with a rack-and-pinion mechanism. In this way the vertical positioning of the spindle is reproducible. The samples are stirred at 10–100 rpm depending on viscosity.

As noted above, the strategy of the experiment is to afford maximum flexibility in choosing the successive steps of equilibration and sampling. Changes in f_{O_2}, in temperature and (in ongoing work which will be reported later) in composition can all be made in a stepwise fashion, and since samples can be taken at any time, the approach to constant state (implying equilibrium) may thus be monitored. Figure 2 illustrates the time-f_{O_2} path of the experiment reported here. The f_{O_2} is changed stepwise by selecting a different gas mixing ratio, following which the response time of the system is a few minutes, as monitored by the oxygen sensors. The entire f_{O_2} history of the experiment is recorded on a chart recorder. Since previous experience with Ir solubility experiments (O'NEILL et al., 1993, 1994) had shown us that equilibrium was reached many times faster on increasing than on decreasing f_{O_2}, the strategy adopted here was to begin the experiment at low f_{O_2}, and then increase f_{O_2} in successive steps. The experiment was then reversed by decreasing f_{O_2}. (However, the results from this experiment show that the kinetics of Ni solution, are quite different from those of Ir. In hindsight, it would have been preferable to conduct the experiment the other way round.)

Some authors have speculated that the gases used to control f_{O_2} may influence Ni solubilities (COLSON, 1992; CAPOBIANCO and AMELIN, 1994). In order to test this hypothesis, and to fix f_{O_2} at lower values than is possible with CO/CO_2 gas mixtures, we have also used H_2/H_2O mixtures. Pure H_2 and a 90% N_2-10% H_2 (forming gas) was bubbled through an ice/water mixture contained in a Dewar flask. The ice/water mixture should control pH_2O at 6.1 mbar. However, for the N_2-H_2 mixture, the oxygen sensor gave a stable e.m.f. indicating log f_{O_2} = −11.80, constant over the time of this segment of the experiment (which lasted for 14 days). This corresponds to a pH_2O of 25.9 mbar, the vapour pressure above water at 21°C, i.e., room temperature. We believe, therefore, that water vapour condensation in our apparatus fixed pH_2O at this level. For the mixture with pure H_2, the oxygen sensor briefly gave a reading corresponding to log f_{O_2} = −13.75, which is precisely that expected for pH_2O = 25.9 mbar. However, the sensor then expired from loss of electrical contact after several minutes of operation. Subsequent examination revealed that the high Rh leg of the thermocouple, which also acts as the
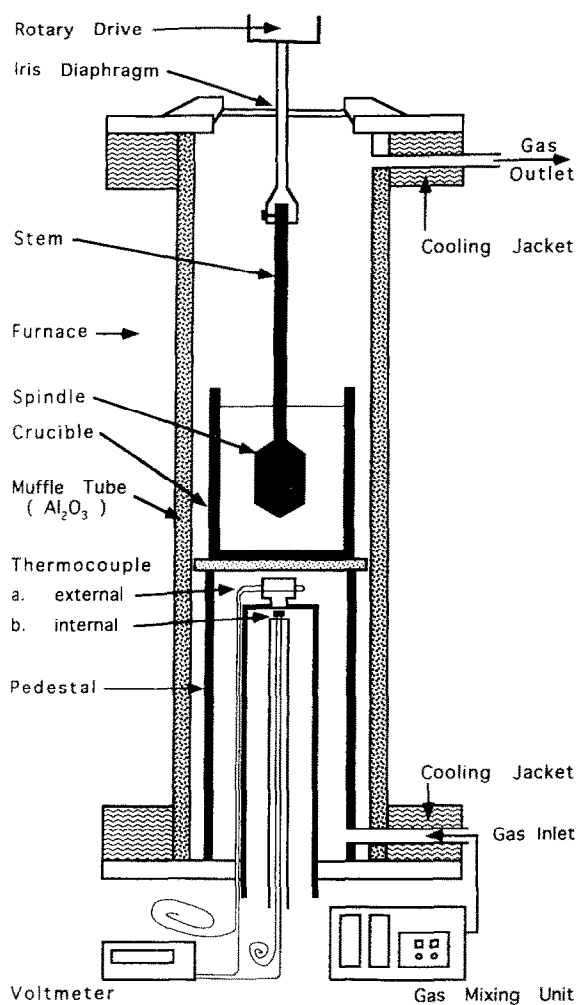

FIG. 1. Schematic illustration of the experiment used to determine the solubility of Ni in a silicate melt. The silicate melt is contained in a crucible of the metal to be dissolved and stirred by a spindle of the same metal. The f_{O_2} is controlled by gas mixtures and monitored by a solid electrolyte cell. The samples are removed with a dip stick through the top of the furnace. See text for further details.

external lead wire, appeared to have melted, suggesting that Rh-rich Rh-Pt alloys may absorb appreciable H_2.

The melts were sampled by stopping the stirring, raising the Ni spindle to a point just above the MgO collar, opening the iris, and dipping an alumina rod (3 mm diameter) into the liquid surface. A drop of melt (typically 0.5 g) congeals around the cool rod. The rod was quickly removed from the furnace, the iris closed, and the rod plunged into distilled water in a beaker. The spindle was lowered back to a position immediately above the melt surface, allowed to thermally equilibrate for 5–10 min, and then lowered into the melt and the stirring resumed.

Analysis

Concentrations of Ni in the samples of quenched melt were analysed at the Bayerisches Geoinstitut in Bayreuth using a ISA-Jobin-Yvon JY 24 sequential Inductively Coupled Plasma–Atomic Emission Spectrometer. Samples were prepared by grinding, overnight drying at 110°C and dissolution in 40% HF. CaF_2 precipitate was dissolved using concentrated H_3BO_3. To these solutions were added 50 ppm of yttrium to serve as an internal standard. The samples were then measured immediately. The ICP-AES was calibrated with 4 single element standard solutions of differing Ni contents. The theoretical accuracy of the analyses is 2% relative.

Concentrations of Ni were analysed at Mainz by instrumental neutron activation analysis (INAA). For INAA irradiations were performed at the TRIGA-reactor of the Institut für Kernchemie at the Johannes-Gutenberg-Universität Mainz, Germany. The neutron flux was 7×10^{11} n cm^{-2} sec^{-1} and duration of radiation 6 h. Samples were counted on large volume Ge(Li)-detectors. Decay of ^{58}Co (for Ni, 810.5 keV, $T_{1/2} = 71$ d) was registered. All samples were counted at least twice. Scandium activities (^{46}Sc, 889.2 KeV and 1120.6 KeV, $T_{1/2} = 84$ d) were simultaneously recorded and used as monitors for INAA procedures.

A comparison of the results from the two analytical methods is given in Fig. 3 and is included in Table 1. The INAA results appear to give slightly higher values at lower concentrations but all samples agree within −10 to +35%, except one (Ni-1-40) for which the ICP analysis is anomalously low. Excluding this sample, the mean deviation difference between the two methods is 12%.

The major element composition of the starting material and of several samples was determined by electron microprobe analysis at the Bayerisches Geoinstitut. The operating conditions were 15 kV accelerating voltage, 15 nA current on brass, 20 s count times, and a defocussed beam. The standards were wollastonite (Ca), enstatite (Mg), spinel (Al), and orthoclase (Si). The composition (normalized to 100%) in weight percent is 26.6% CaO, 10.7% MgO, 15.3% Al_2O_3, and 47.4% SiO_2. There was no drift of composition during the course of the experiment.

RESULTS AND DISCUSSION

Kinetics

Sampling at each condition of f_{O_2} has been performed in a time series. An example of data for these time series is presented in Fig. 4, where it is evident that the time required to reach a steady state after lowering f_{O_2} (and Ni solubility) is shorter than after raising f_{O_2}. The higher rate of equilibration in the direction of decreasing Ni content is consistent with the observation made during similar experiments involving the reduction of Fe in Fe-rich melts (DINGWELL and VIRGO, 1987), i.e., the rate of reduction was observed to be much higher than the rate of oxidation. The explanation proposed at that time was that the reduction proceeds by generation of oxygen gas, which forms bubbles which are easily liberated from the melt. The oxidation of the same melt requires diffusive transport of oxygen. Although this is assisted in these experiments by forced convection, this latter process should still be slower than the former. This asymmetry in

the kinetics is in the opposite sense to that observed by us for oxidation and reduction of Ir-bearing melts (O'NEILL et al., 1993, 1994), where the rate of decrease of Ir concentration on lowering f_{O_2} is orders of magnitude slower than the rate of increase on raising f_{O_2}. The indication is that a quite different mechanism controls the rate of reduction in the Ir experiments. This mechanism may be related to differences in the absolute concentration ranges of the dissolved metals (ppm in the Ni experiment, ppb in the Ir study), or to differing surface properties of the metals affecting particle suspension properties at high temperatures. An understanding of these kinetics may be important for the interpretation of other metal solubility studies, and warrants further investigation.

f_{O_2} and Temperature Dependence of Nickel Solubility

The analysed Ni contents of our samples (from both INAA and ICP-AES), together with the f_{O_2} derived from oxygen specific electrode measurements, the elapsed time of the experiment and the temperature, are presented in Table 1. As noted above, the sequence of the experimental conditions is also graphically portrayed in Fig. 2. The experiment began with an equilibration at very low f_{O_2} and 1300°C using the lowest CO_2/CO ratio at which a nearly stable f_{O_2} as measured by the sensor, could be empirically obtained. The flow rate of CO_2 in this mixture was below the calibration threshold of the mass flow controllers. The f_{O_2} was increased stepwise by changing the CO_2/CO ratio up to the highest value of f_{O_2} investigated here. Next the f_{O_2} was reduced to provide a reversal. The experiment was then switched to the $N_2-H_2-H_2O$ mixture, and then further reduced to an extremely low value using the pure H_2-H_2O mix. Finally, the f_{O_2} was increased again in preparation for investigation of the temperature dependence of solubility. The temperature dependence was determined during stepwise increase of the temperature from 1270 to 1390°C at 30°C intervals, at constant gas mixing ratio ($CO_2/CO = 1$).

The information on the rate of approach to equilibrium from the time series at constant f_{O_2} (e.g., Fig. 4) indicates that, especially during the earlier part of the experiment, equilibrium solubility of Ni at 1300°C should be approached but not quite attained. Our results thus consist of reversals brackets, which constrain the equilibrium solubility of Ni to lie either above them (increasing f_{O_2}) or below them (decreasing f_{O_2}). This is illustrated in Fig. 5.

The equilibrium solubility of Ni in a silicate melt of fixed composition may be described by the expression

log (Ni solubility in ppm)

$$= x \log f_{O_2} + C_1/T(K) + C_2, \quad (1)$$

where x is the formal valence of Ni in the melt, according to the balanced chemical reaction

$$Ni_{(metal)} + x/4 \, O_2 = Ni_{x/2}O_{(melt)}.$$
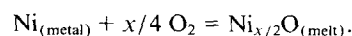
Thus, x may be determined from the slope of a plot of log (Ni solubility in ppm) vs. log f_{O_2}. As shown in Fig. 5, our data can be well fitted using $x = 2$; that is, assuming Ni dissolves only in the silicate melt as Ni^{2+}. There is no need to postulate the existence of any zero-valent Ni (Ni^0) dissolved in the melt. In fact, the minimum slope which still
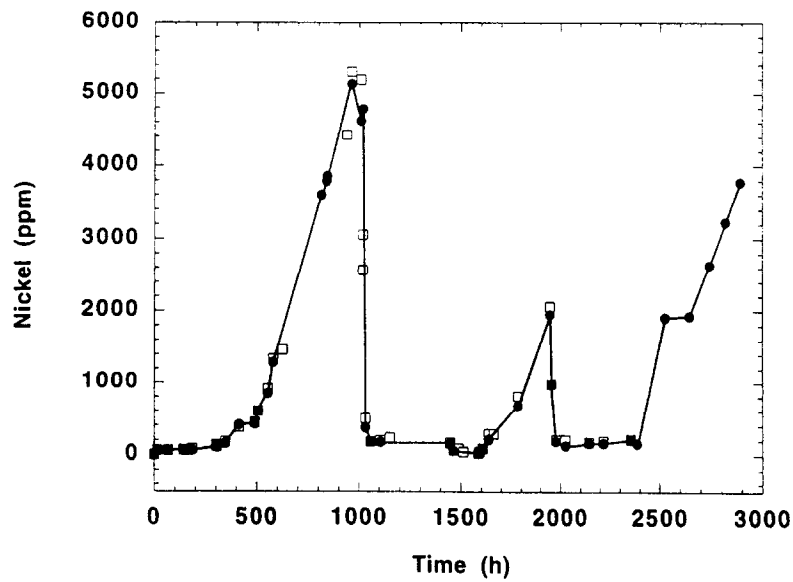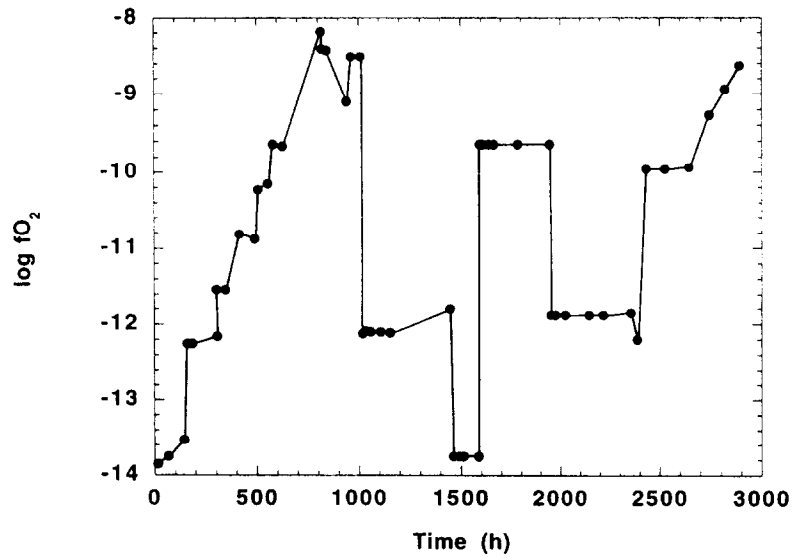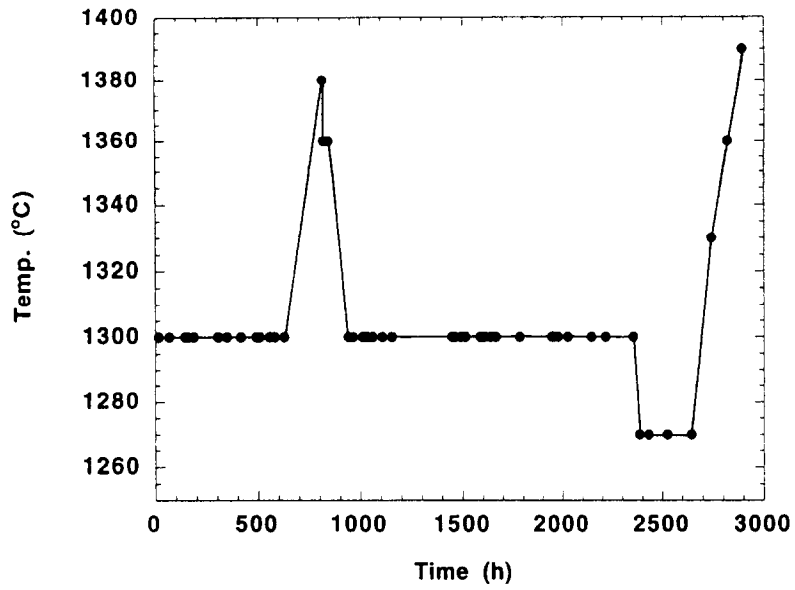
satisfies the reversal brackets is 0.46, and the maximum amount of Ni^0 is constrained to be less than ~ 10 ppm.

The temperature dependence of the solubility of Ni is presented in Fig. 6a where the experimental data obtained at a constant CO/CO_2 ratio of 1 are shown. A combined fit of these data and the reversal brackets of Fig. 5 to an expression with the form of Eqn. 1, assuming $x = 0.5$, gives

log (Ni solubility in ppm)

$$= 0.5 \log f_{O_2} + 7670/T(K) + 3.28, \quad (3)$$

with an estimated accuracy of ± 0.05 in log Ni (equivalent to $\pm 12\%$ in Ni) over most of the T-f_{O_2} range covered by the experiment.

Note that the solubility of Ni decreases at constant f_{O_2} with increasing temperature, implying that, at constant f_{O_2}, the partition coefficient of Ni between metal and silicate melt $(D_{Ni}^{met/sil\ melt})$ will increase with increasing temperature.

Our results are in essentially perfect agreement with those of HOLZHEID et al. (1994) for a anorthite-diopside eutectic composition at higher f_{O_2} values as shown in Fig. 5. At lower f_{O_2} values we infer slightly lower solubilities, which provide tighter constraints on the maximum amount of Ni^0. The temperature dependence of the Ni solubility in Eqn. 3 is also the same as that found by HOLZHEID et al. (1994).

These data are compared with data for Ni solubility reported by COLSON (1992) in a melt of the 1 atm eutectic in the system $CaAl_2Si_2O_8$-$CaMgSi_2O_6$ at 1400°C and in a similar range of f_{O_2} (Fig. 5). At high f_{O_2} both studies concur in the observation of a slope corresponding to the solution of Ni almost entirely as Ni^{2+}. At low f_{O_2}, the results of COLSON (1992) deviate from this trend towards a lower slope value; a smaller dependence of Ni content on f_{O_2}. COLSON (1992) interpreted this trend as resulting from the presence of neutral Ni (Ni^0) dissolved in these melts at low f_{O_2}. Our data show no such deviation from the behavior expected of Ni dissolved in the divalent (Ni^{2+}) state to the lowest values of f_{O_2} that we have been able to obtain. The amount of Ni^0 expected at 1300°C from Eqn. 6 of COLSON (1992) would be 300 ppm.

How can we explain the difference between our results and those of COLSON (1992)? In his interpretation of his experimental observations, Colson supposed that the apparent decrease of Ni as analysed by the electron microprobe away from the Ni metal-silicate glass interface was due to continuous volatile loss of Ni from the silicate melt. In fact, thermodynamic data for possible Ni gas species (BARIN, 1989—including Ni carbonyls, which are only stable at low temperatures) reveal no tendency for any appreciable Ni volatility. In agreement with this expectation, we observe absolutely no evidence for any Ni volatility in our experiment, even after 3000 h under conditions similar to those used in the experiments of COLSON 1992; in which drastic loss of Ni is claimed to be observable in a matter of minutes. The possibility needs to be entertained that the "diffusion profiles"
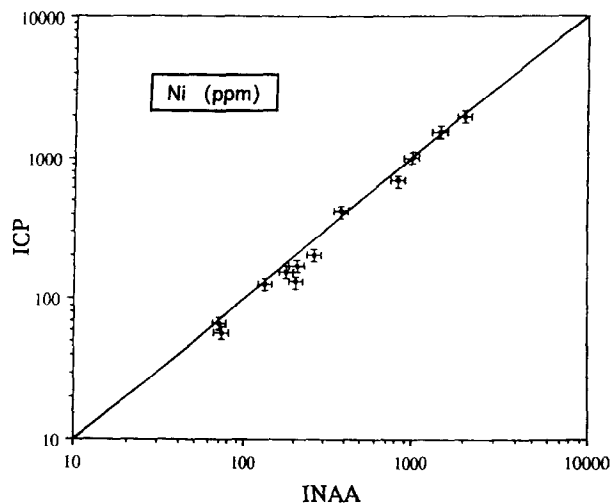

FIG. 3. A comparison of the analytical data for Ni determined by ICP-AES (Bayreuth) and INAA (Mainz).

of COLSON (1992) are analytical artifacts caused by secondary X-ray fluorescence and the proximity of the Ni metal, as has recently been experimentally demonstrated to operate over comparable distances by CAPOBIANCO and AMELIN (1994; see their Fig. 1). The true levels of Ni in the experiments of COLSON (1992) may simply be those found more than 200 μ from the metal interface.

Other possible explanations for higher than expected levels of Ni or other siderophile elements in silicate melts at low f_{O_2}, which could give rise to thoughts of neutral metal species, are

1) Very small particles of metal may be stranded by suspension in the melt, and unable to settle out on normal experimental timescales. Here we hope that the mechanical stirring which sets up a forced convective regime in the liquid sweeps metal particles to the crucible walls. When attempting to measure the solubility of metals at very low levels, it is also important to demonstrate reversal of the equilibrium not only by starting with high and low levels of the metal in the melt, but also by demonstrating that the steady state is actually being *approached* from the high and low levels. The ability to do this by taking samples in a time series is perhaps the principal strength of the experimental method described here. The need for this kind of demonstration would be particularly important if there is asymmetry in the rates of increase and decrease of metal concentrations (as found for Ir; e.g., see O'NEILL et al., 1993, 1994): if the rate of increasing metal concentration is rapid, absorbed oxygen in the starting materials may produce significant levels of the metal in the melt initially, even in nominally metal-free

FIG. 2. The sequence of events in the Ni solubility experiment. Temperature, f_{O_2} fugacity, and analysed Ni content are plotted vs. time. The experiment began at 1300°C under very reducing conditions. The f_{O_2} was systematically increased in a stepwise fashion and the melt was continually sampled. Reversals in the Ni contents were achieved through subsequent reduction of the f_{O_2}. Finally the f_{O_2} was held constant at the temperature was varied. See text for more details.

D. B. Dingwell et al.

Table 1. Experimental Results

Sample Nr.	Time (h)	Temp. (°C)	CO_2 (%)	log fO_2 (a)	emf (mV)	log fO_2 (b)	Ni INAA (ppm)	Ni ICP (ppm)
1	16	1300	<5		1028	-13.85	64	67
2	66	1300	<5		1020	-13.75	62	57
3	143	1300	<5		1003	-13.53	73	57
4	159	1300	5	-12.28	903	-12.25	68	59
5*	184	1300	5	-12.28	903	-12.25	82	63
6	304	1300	5	-12.28	896	-12.16	114	102
7	302	1300	10	-11.63	848	-11.55	134	127
8*	346	1300	10	-11.63	848	-11.55	180	154
9*	414	1300	20	-10.93	791	-10.82	380	410
10	490	1300	20	-10.93	796	-10.88	440	420
11	506	1300	35	-10.26	745	-10.23	600	600
12	554	1300	35	-10.26	739	-10.15	920	850
13	579	1300	50	-9.72	699	-9.64	1340	1290
14*	626	1300	50	-9.72	701	-9.66	1470	
15	814	1380	67	-8.19	616	-8.19		3600
16	819	1360	67	-8.43	626	-8.41		
17	840	1360	67	-8.43	628	-8.43		3790
18*	843	1360	67	-8.43	628	-8.43		3860
19	939	1300	67	-9.11	657	-9.10	4430	
20	961	1300	80	-8.52	611	-8.51	5300	5130
21	1008	1300	80	-8.52	611	-8.51	5190	4620
22a	1018	1300	5	-12.28	893	-12.12	2570	4790
22b	1018	1300	5	-12.28	893	-12.12	3060	
23	1033	1300	5	-12.28	890	-12.09	500	370
24	1058	1300	5	-12.28	891	-12.10	182	182
25	1106	1300	5	-12.28	891	-12.10	200	178
26	1153	1300	5	-12.28	892	-12.11	240	
27a	1447	1300	(c)		868	-11.80	163	
27b	1447	1300	(c)		868	-11.80	173	162
28	1464	1300	(d)		1020	-13.75	71	67
29	1491	1300	(d)				96	
30	1513	1300	(d)				50	
31	1587	1300	(d)				32	25
32	1594	1300	50	-9.72			52	39
33	1608	1300	50	-9.72			94	92
34a	1638	1300	50	-9.72			270	210
34b	1638	1300	50	-9.72			290	220
35	1663	1300	50	-9.72	699	-9.64	290	
36	1783	1300	50	-9.72			820	680
37	1946	1300	50	-9.72			2060	1950
38	1954	1300	5	-12.28			990	990
39	1977	1300	5	-12.28			210	192
40	2025	1300	5	-12.28			210	131
41	2144	1300	5	-12.28			180	170
42	2217	1300	5	-12.28	874	-11.88	194	170
43	2355	1300	5	-12.28	872	-11.85	220	210
44	2386	1270	5	-12.64	882	-12.20		158
45	2432	1270	50	-10.09	710	-9.96		
46	2526	1270	50	-10.09	710	-9.96		1910
47	2645	1270	50	-10.09	709	-9.94		1930
48*	2742	1330	50	-9.38	683	-9.27		2640
49	2818	1360	50	-9.04	669	-8.94		3230
50	2890	1390	50	-8.72	656	-8.63		3780

(a) calculated from the gas mixing ratio
(b) calculated from the oxygen sensor emf
(c) $H_2O-H_2-N_2$
(d) H_2O-H_2
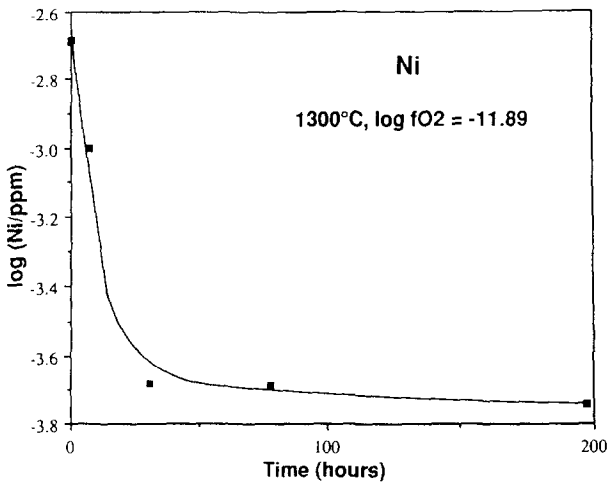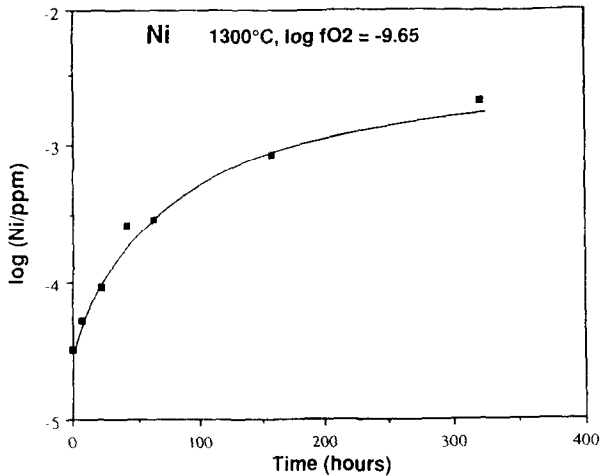* Experiment was temporarily interrupted after these samples were taken, and then restarted

FIG. 4. The approach to equilibrium in Ni content for melts undergoing oxidation and reduction. The oxidation proceeds much more slowly than the reduction (note the different scales).
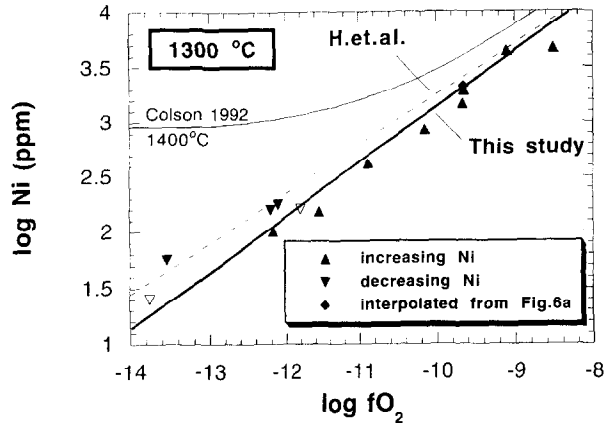

FIG. 5. Reversals of the equilibrium solubility of Ni in the investigated melt at 1300°C, as a function of f_{O_2} from $10^{-8.5}$ to $10^{-13.75}$. The best fit line is drawn assuming a slope of 0.5 (all Ni as Ni^{2+}) and has been constrained to satisfy also the solubility-temperature data (shown in Fig. 6). The line labelled "H et al." is calculated for a temperature of 1300°C from the fit to their data of HOLZHEID et al. (1994), for a Di-An eutectic melt. Closed symbols = CO-CO_2 mixtures; open symbols = H_2O-$H_2 \pm N_2$ mixtures.

silicate, which may then not decrease during the timescale of the experiment.

2) Very low f_{O_2} conditions are difficult to produce experimentally using C-based gas mixtures, not least because graphite precipitation in the cooler parts of the furnace may alter the composition of the mixture. H_2-rich CO_2-H_2 gases may fail to equilibrate at high flow rates, and are liable to unmixing at low flow rates from thermal diffusion (HUEBNER, 1987). Electrochemical oxygen sensors provide some safeguard against these potential pitfalls, but may perhaps not be infallible. Their response is catalysed by their Pt surface, and could thus record the expected f_{O_2} for the gas mixture, whereas the f_{O_2} actually experienced by the rest of the experiment might be modified by processes such as carbon precipitation or unmixing operating over longer timescales. Here we have guarded against such difficulties by also using H_2-H_2O mixtures.

3) Attempting chemical analyses with a method near to its limit of detection is fraught with difficulty, and often re-

sults in erroneously high levels of the element sought. In the case of Ni, a good example is provided by its determination in pallasitic olivines: REED et al. (1979) showed that ion microprobe analysis gave concentrations of
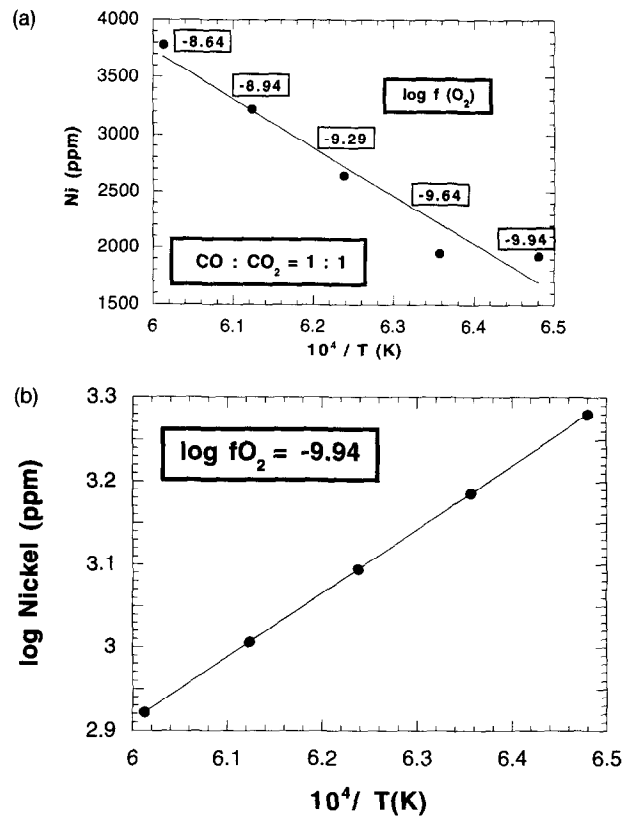

FIG. 6. (a) The temperature dependence of the solubility of Ni in the melt at a constant gas-mixing ratio of CO/CO_2 = 1:1. (b) The calculated temperature dependence of solubility at a constant f_{O_2}.

22–41 ppm, considerably lower than the earlier electron microprobe analyses of 40–70 ppm (although subsequent electron probe analyses by REED et al. (1979) were in agreement with the ion probe data.). In this study we have avoided this problem, since our samples are large enough for analysing using methods suitable for low levels, and we have checked one method against the other on the same samples. A potentially useful byproduct of the present experiments is that our samples could also make useful standards for microbeam techniques.

SUMMARY

We present a new experimental strategy for the determination of metal solubilities in silicate melts at conditions of controlled and variable temperature, f_{O_2}, and composition. This method is extremely flexible. Composition, f_{O_2} and temperature can be changed in any direction. Sampling is simple and provides enough material for chemical analyses using methods well suited for the determination of low levels. The reversibility of equilibria may be unambiguously demonstrated by following the approach to a steady state in through a time series of samples. Our results for the solubility of Ni in a silicate melt disagree with previous determinations of the solubility of Ni in an anorthite-diopside melt at low f_{O_2} (COLSON, 1992) but agree with the results of HOLZHEID et al. (1994) on that melt composition.

Editorial handling: G. Faure

REFERENCES

BARIN I. (1989) *Thermochemical Data of Pure Substances.* Vol. 1 and 2. VCH, Weinheim, Germany.

CAPOBIANCO C. J. and AMELIN A. A. (1994) Metal-silicate partitioning of nickel and cobalt: The influence of temperature and oxygen fugacity. *Geochim. Cosmochim. Acta* 58, 125–140.

COLSON R. O. (1992) Solubility of neutral nickel in silicate melts and implications for the Earth's siderophile element budget. *Nature* 357, 65–68.

DINGWELL D. B. and VIRGO D. (1987) The effect of oxidation state on the of melts in the system Na_2O-FeO-Fe_2O_3-SiO_2. *Geochim. Cosmochim. Acta* 15, 195–205.

DINGWELL D. B., O'NEILL H. ST.C., PALME H., and SPETTEL B. (1993) The oxidation state of Ni in silicate melts at low f_{O_2}. *Eos* 74, 338.

EHLERS K., GROVE T. D., SISSON T. W., RECCA S. I., and ZERVAS D. A. (1992) The effect of oxygen fugacity on the partitioning of nickel and cobalt between olivine, silicate melt, and metal. *Geochim. Cosmochim. Acta* 56, 3733–3743.

HOLZHEID A., BORISOV A., and PALME H. (1994) The effect of oxygen fugacity and temperature on solubilities of Ni, Co, and Mo in silicate melts. *Geochim. Cosmochim. Acta* 58, 1975–1981 (this issue).

HUEBNER J. S. (1987) Use of gas mixtures at low pressures to specify oxygen and other fugacities of furnace atmospheres. In *Hydrothermal Experimental Techniques* (ed. G. C. ULMER and H. L. BARNES), pp. 20–60. Wiley.

MORSE S. A., RHODES J. M., and NOLAN K. M. (1991) Redox effect on the partitioning of nickel in olivine. *Geochim. Cosmochim. Acta* 55, 2373–2378.

O'NEILL H. ST.C., DINGWELL D. B., PALME H., and SPETTEL B. (1993) The solubility of Ir in silicate melts and Ir metal/melt distribution coefficients. *Eos* 74, 338.

O'NEILL H. ST.C., DINGWELL D. B., BORISOV A., SPETTEL B., and PALME H. (1994) Experimental petrochemistry of some highly siderophile elements at high temperatures, and some implications for core formation and the mantle's early history. *Lithos* (in press).

REED S. J. B., SCOTT E. R. D., and LONG J. V. P. (1979) Ion microprobe analysis of olivine in pallasite meteorites for nickel. *Earth Planet. Sci. Lett.* 43, 5–12.

STEELE A. M., COLSON R. O., KOROTEV R. L., and HASKIN L. A. (1992) Apollo 15 green glass: Compositional distribution and petrogenesis. *Geochim. Cosmochim. Acta* 56, 4075–4090.